to the ninth fluorine shell (nineteenth shell counting both F and Na nuclei). This corresponds to 236 F nuclei. For both types of single sum the contribution from the remainder of the spins in the lattice is estimated by an isotropic integration. This is less than 1.0% in each case. The integrated contribution to the single sum of type $P_{j\alpha}{}^4$ is less than 0.005%. Integrated contributions to the double or triangular sums have not been calculated. From the convergence of the lattice sums, we estimate that the asymptotic value differs from our truncated value by less than 10%.

The lattice sums required to evaluate all the quantities appearing in this paper are presented in Table I. Using these results, the numerical values of the quantities appearing in Secs. II A and II B have been calculated and are given in Table II.

PHYSICAL REVIEW B VOLUME 1, NUMBER 5 1 MARCH 1970

# Comparison of Average-Potential Models and Binary-Collision Models of Axial Channeling and Blocking

J. U. ANDERSEN AND L. C. FELDMAN
*Bell Telephone Laboratories, Murray Hill, New Jersey 07974*
(Received 26 June 1969)

A comparison is made of three types of calculations of the axial "channeling dip": the large decrease in yield of close-encounter processes for energetic ions incident on a single crystal parallel to a low-index direction. The models, indicated as (1) the binary-collision model, (2) the halfway-plane model, and (3) the continuum model, are used to calculate the dip for two standard cases corresponding to recent experiments. The methods are compared as to treatment of potential and treatment of thermal vibrations. The ease of calculation versus quantitative accuracy for the different methods is discussed, and finally the agreement with experimental results is briefly reviewed.

## INTRODUCTION

ONE of the most striking and useful channeling effects observed is the almost complete extinction of close-encounter processes for energetic ions incident on a single crystal parallel to a low-index direction. A large amount of experimental information is becoming available on this "string effect," for a variety of combinations of $Z_1$, $Z_2$, $E$, and $T$, where $Z_1$ and $Z_2$ are the atomic numbers of the incident particles and the crystal atoms, respectively, $E$ is the particle energy, and $T$ is the crystal temperature.

Several authors[1–5] have contributed to the understanding of this phenomenon in terms of the motion of channeled particles in an average string, or row, potential. The most detailed and comprehensive treatment has been given by Lindhard,[3] and Linhard *et al.*[6] The important question of applicability of classical mechanics was discussed, and it was concluded that for channeling of heavy particles (protons, $\alpha$-particle, etc.) classical orbital pictures may be used. From a discussion of the validity of the continuum model, simple estimates of the critical angle resulted. An important modification to the continuum model is the halfway-plane description introduced in Appendix A of Ref. 3. On the basis of this description and a simple model for the influence of thermal vibrations, formulas for the angular distribution of particles emitted from a string atom were obtained. These "blocking" formulas also apply to channeling experiments, where the yield of a close-encounter process is measured as a function of incidence angle of the beam with respect to a string direction. This is a consequence of the rule of reversibility as discussed in Ref. 3. Recently, a systematic numerical evaluation of these formulas has been made.[7,8]

Some of the early blocking results[9,10] were interpreted in terms of a simple two-body model, where the emitted particle only interacts with the nearest neighbor on the string. The use of high-speed computers has made it possible to extend this two-body model and take into account binary collisions with all string atoms. Thermal vibrations may be taken into account by letting all string atoms vibrate independently. Such calculations

[1] R. S. Nelson and M. W. Thomson, Phil. Mag. **8**, 1677 (1963).
[2] C. Lehmann and G. Leibfried, J. Appl. Phys. **34**, 2821 (1963).
[3] J. Lindhard, Kgl. Danske Videnskab. Selskab, Mat.-Fys. Medd. **34** (1965).
[4] C. Erginsoy, Phys. Rev. Letters **15**, 360 (1965).
[5] A. F. Tulinov, Dokl. Akad. Nauk SSSR **162**, 546 (1965) [English transl.: Soviet Phys.—Doklady **10**, 463 (1965)].
[6] P. Lervig, J. Lindhard, and V. Nielsen, Nucl. Phys. **A96**, 481 (1967).
[7] J. U. Andersen, Kgl. Danske Videnskab. Selskab, Mat.-Fys. Medd. **36** (1967).
[8] Because of the finite step size in the integration, an error of ~5% was inherent in these calculations. In more accurate calculations, the width is increased by $\sim 0.05\psi_1$. This explains the small discrepancy between results in this paper and those in Ref. 7.
[9] D. S. Gemmel and R. E. Holland, Phys. Rev. Letters **14**, 945 (1965).
[10] O. S. Oen, Phys. Letters **19**, 358 (1965).

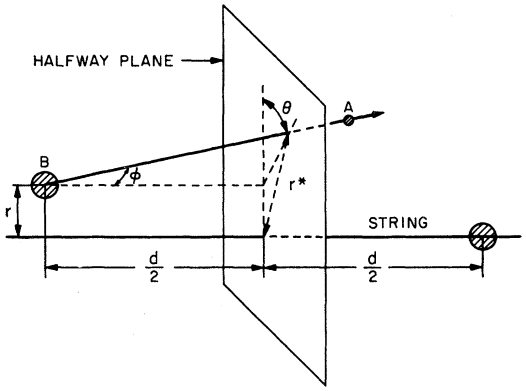


FIG. 1. Emission of particle from string atom and geometry for the halfway-plane calculation.

have now been performed by several authors.[11–14] In this paper, we estimate the relative merits of these different types of calculations. The calculations are all based on classical mechanics and consider only the interaction of the emitted particle with one isolated row of atoms.

A detailed comparison between Monte Carlo calculations and Lindhard's analytical theory, with a somewhat different scope, has recently been published.[12]

## NUMERICAL HALFWAY-PLANE CALCULATION

The calculations in Ref. 7 are based on the formulas given by Lindhard.[3] These formulas are derived from conservation of transverse energy at the planes halfway between string atoms. The transverse energy $E_\perp$ is the energy associated with the motion of the particle projected on a plane, perpendicular to the string. As shown in Ref. 3, $E_\perp$, given by

$$E_\perp = E\varphi^2 + U(r), \tag{1}$$

is approximately conserved in a collision between the particle and a string when measured at the halfway planes, provided that the particle is approaching the string at a small angle. Here, $\varphi$ is the angle between the particle velocity and the string and $U(r)$ is the continuum-string potential given as a function of the distance $r$ from the string by

$$U(r) = \frac{1}{d}\int_{-\infty}^{\infty} dz\, V[(r^2+z^2)^{1/2}], \tag{2}$$

where $V(R)$ is the particle-atom potential and $d$ is the spacing of atoms in the string.

On the basis of this conservation, the angular distribution of particles emitted isotropically from a string atom is calculated as illustrated in Fig. 1. The particle A with energy $E$ is emitted from atom B, the angle of emission is $\varphi$, and $\vartheta$ is the azimuthal angle of emission. At the moment of emission, the atom B is at a distance $r$ from an otherwise perfect string. Thus, the thermal vibrations of all string atoms except the emitting atom are neglected, whereas the thermal vibrations of atom B are represented by a probability distribution for $r$, $dP(r)$, which is taken as a Gaussian

$$dP(r) = e^{-r^2/\rho^2}[d(r)^2/\rho^2]\alpha, \tag{3}$$

where $\alpha \simeq 1$ is a normalization constant and $\rho^2$ is the mean square displacement perpendicular to the string.

The emission is assumed to be isotropic. Consequently, the probability distribution for $\varphi$ is proportional to $\sin\varphi \simeq \varphi$ and for $\vartheta$ is a constant. The transverse energy of the particle is calculated at the halfway plane according to (1).

From this, the following expression for the distribution in transverse energy[15] is derived:

$$\Pi(E_\perp) = \int_{r=0}^{r_0} dP(r) \int_0 d(E\varphi^2) \times \int_0^{2\pi} \frac{d\vartheta}{2\pi} \delta(E_\perp - U(r^*) - E\varphi^2), \tag{4}$$

where $\delta(E_\perp)$ is the usual $\delta$ function. Here, $r_0$ is given by $\pi r_0^2 = (Nd)^{-1}$, where $N$ is the number of atoms per unit volume.

Assuming conservation of $E_\perp$ during the passage of the particle through the crystal and neglecting the change of $E_\perp$ due to the transmission through the crystal surface,[16] we get the angular distribution outside the crystal from (4) through the relation $E_\perp = E\psi_e^2$ between the transverse energy and the emergence angle.

In Ref. 7, Eq. (4) was evaluated numerically by simulating, according to Fig. 1, the emission of particles from a string atom, and varying independently the parameters $r$, $\varphi$, and $\vartheta$. Linhard's standard potential was used:

$$U(r) = (Z_1 Z_2 e^2/d)\ln[(Ca/r)^2+1]. \tag{5}$$

Here, $d$ is the spacing between atoms in the string, $Z_1$ and $Z_2$ are the atomic numbers of the particle and the atoms, respectively, $C$ is a potential constant taken to be $\sqrt{3}$, and $a$ is the Thomas-Fermi radius[17]

$$a = 0.8853 a_0 (Z_1^{2/3} + Z_2^{2/3})^{-1/2}. \tag{6}$$

The average potential (5) corresponds to the following atomic potential:

$$V(R) = (Z_1 Z_2 e^2/R)[1 - R/(R^2+C^2a^2)^{1/2}]. \tag{7}$$

[11] L. C. Feldman, Ph.D. thesis, Rutgers University, 1966 (unpublished).
[12] D. V. Morgan and D. Van Vliet, Can. J. Phys. **46**, 503 (1968).
[13] J. H. Barrett, Phys. Rev. **166**, 219 (1968).
[14] I. M. Torrens and L. T. Chadderton, Can. J. Phys. **46**, 1303 (1968).
[15] $\Pi(E_\perp)$ is normalized to unity in the random case, i.e., for $U(r) \equiv 0$.
[16] In Ref. 7, it is shown that the surface transmission does not change the width of the dip appreciably.
[17] J. Lindhard, V. Nielsen, and M. Scharff, Kgl. Danske Videnskab. Selskab, Mat.-Fys. Medd. **36** (1968).

For a discussion of the standard potential (4), the reader is referred to Refs. 3 and 17. Another widely used[4] potential is the Molière approximation to the Thomas-Fermi potential

$$V(R)=(Z_1Z_2e^2/R)(0.1e^{-6R/a}+0.55e^{-1.2R/a}+0.35e^{-0.3R/a}), \quad (8)$$

which leads to the following expression for the average potential:

$$U(r)=(2Z_1Z_2e^2/d)[0.1K_0(6r/a)+0.55K_0(1.2r/a)+0.35K_0(0.3r/a)], \quad (9)$$

where $K_0$ is the zeroth-order modified Bessel function of the second kind.

In the continuum approximation, the transverse energy is assumed to be conserved along the whole trajectory, not only at the halfway planes. In this approximation, the formula corresponding to Eq. (4) is obtained by setting $r^*=r$. Equation (4) then reduces to

$$\Pi(E_\perp)=\int^{r_0} dP(r)\Big|_{U(r)>E_\perp}. \quad (10)$$

Setting $r^*=r$ in (4) amounts to neglecting terms in $r^*$ of relative magnitude $\sim\varphi d/\rho$. A reasonable criterion for the validity of the continuum approximation is then

$$\rho/\psi_1 d>1, \quad (11)$$

since $\varphi\lesssim\psi_1$. [See Eqs. (15) and (16).]

When $dP(r)$ is given by (3), (10) reduces to

$$\Pi(E_\perp)=e^{-r^2/\rho^2}-e^{-r_0^2/\rho^2}, \quad (12)$$

evaluated at $U(r)=E_\perp$. The last term may usually be neglected since $\rho\ll r_0$. This formula then leads to the following expression for the half-width at half-dip:

$$\psi_{1/2}=\{U[\rho(\ln 2)^{1/2}]/E\}^{1/2}. \quad (13)$$

When the standard potential (5) is inserted, we get simple analytical expressions[3] for $\Pi(E_\perp)$ and $\psi_{1/2}$:

$$\Pi(E_\perp)\cong\exp[-(C^2a^2/\rho^2)(e^{2E_\perp/E\psi_1^2}-1)^{-1}], \quad (14)$$

$$\psi_{1/2}=\psi_1\{\tfrac{1}{2}\log[C^2a^2/\rho^2)(1/\log 2)+1]\}^{1/2}. \quad (15)$$

The last term in (12) has been neglected. $\psi_1$ is given by

$$\psi_1=(2Z_1Z_2e^2/d\times E)^{1/2}. \quad (16)$$

Erginsoy[18] has suggested taking into account the vibrations of all string atoms except the emitting atom, by averaging the continuum potential $U(r)$ over the probability distribution (3) of the string atoms:

$$U_T(r)=\int dP(\mathbf{r}')U(|\mathbf{r}-\mathbf{r}'|). \quad (17)$$

Introducing the standard potential (5) and the probability distribution (3) ($\alpha=1$), we get

$$U_T(r)=\frac{Z_1Z_2e^2}{d}\int_0\frac{d(r'^2)}{\rho^2}\times e^{-r'^2/\rho^2}\int_0^\pi\frac{d\vartheta}{\pi}\ln\left(\frac{C^2a^2}{r^2+r'^2-2rr'\cos\vartheta}+1\right). \quad (18)$$

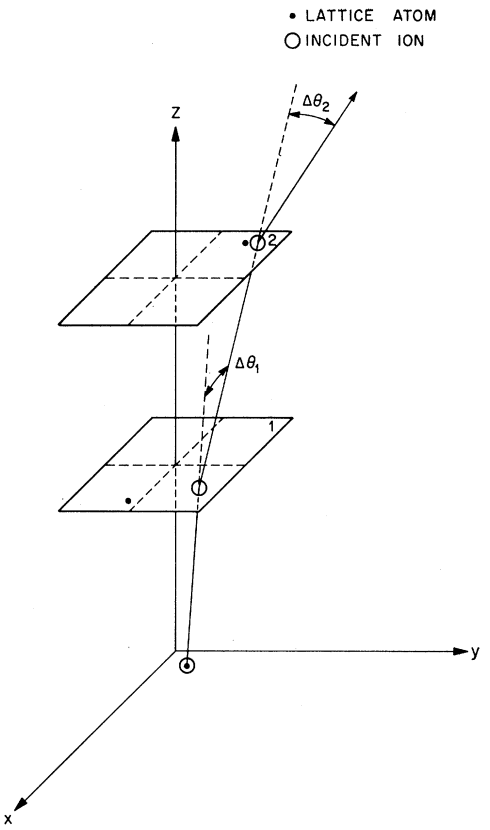


FIG. 2. Emission of particle from string atom and geometry for the binary-collision calculation.

## BINARY-COLLISION CALCULATION

In the binary-collision model, the interaction between the particle and a row of atoms is calculated by treating each scattering individually as a binary collision. The calculation follows particles "emitted" (originating) from a lattice site at small angles to a string. The string or row consists of scattering centers (atoms) vibrating independently about their equilibrium positions according to a Gaussian position distribution. The origin or emitting atom is also allowed to vibrate and is further assumed to emit the particles isotropically. The particles are allowed to scatter from each of up to 100 atoms in the string or until certain cutoffs are reached in the impact parameter or emerging angle. The final result of many different particle trajectories consists of an angular distribution around the symmetry axis.

[18] B. R. Appleton, C. Erginsoy, and W. M. Gibson, Phys. Rev. **161**, 330 (1967).

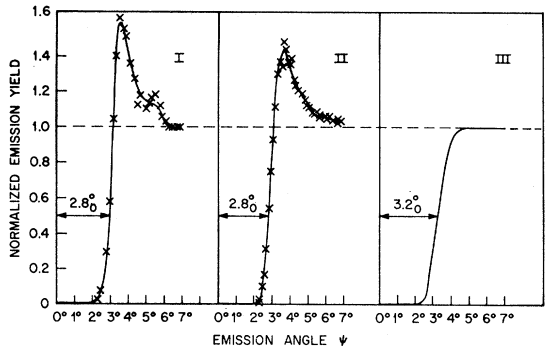


FIG. 3. The calculated [100] dips in W at 0°K for 400-keV protons in the (I) binary-collision model (single atom vibrating), (II) halfway-plane model, and (III) continuum model.

The method of the calculation is shown schematically in Fig. 2. The string of atoms is along the $z$ axis and the particle is emitted in some initial plane. In the static case (no vibrations), the emerging particle remains in this plane and the problem is two-dimensional; however, when vibrations are included, there may be a component of the particle-atom force which scatters the particle from its initial plane.

For a particular scattering, we are interested in the quantity $\Delta\mathbf{P}=(\Delta P_x,\Delta P_y)$, the momentum transfer in the $x$-$y$ plane. This quantity is given by

$$\Delta\mathbf{P}=\int_{-\infty}^{\infty}\mathbf{F}dt, \tag{19}$$

where $\mathbf{F}$ is the projection on the $x$-$y$ plane of the force on the particle and the integral is over the complete time of the trajectory. The momentum transfer for a single small-angle scattering may also be expressed in terms of the average potential

$$\Delta\mathbf{P}=\frac{1}{v}\int_{-\infty}^{\infty}dz\boldsymbol{\Delta}_{\mathbf{r}}V[(z^2+r^2)^{1/2}] \tag{20}$$

or

$$\Delta\mathbf{P}=\frac{d}{v}\frac{\partial}{\partial r}U(r)\cdot\frac{\mathbf{r}}{r}, \tag{21}$$

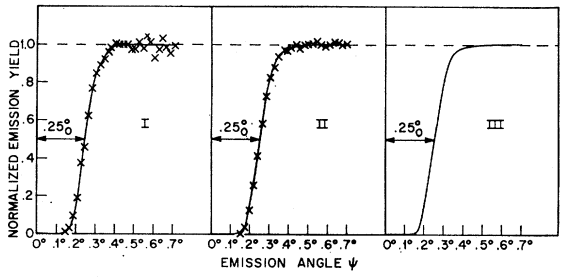


FIG. 4. The calculated [110] dips in Si at 300°K for 7-MeV protons in the (I) binary-collision model (single atom vibrating), (II) halfway-plane model, and (III) continuum model.

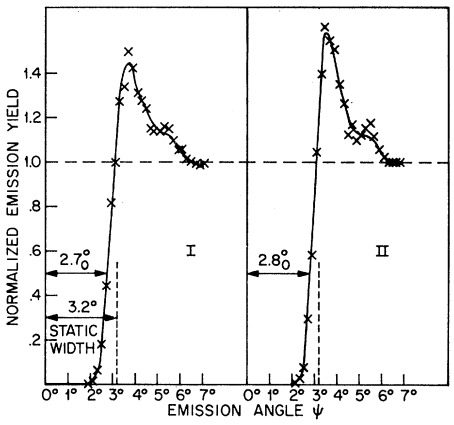


FIG. 5. The calculated [100] dips in W at 0°K for 400-keV protons in the binary-collision model with (I) all atoms vibrating and (II) single atom vibrating.

where

$$U(r)=\frac{1}{d}\int_{-\infty}^{\infty}dzV[(z^2+r^2)^{1/2}] \tag{22}$$

is the average potential defined in the previous section, $v$ is the magnitude of the particle velocity, and $r$ is the impact parameter for the scattering $\mathbf{r}=(x,y)$. The deflection $\boldsymbol{\Delta}\theta=(\Delta\theta_x,\Delta\theta_y)$ is given by

$$\boldsymbol{\Delta}\theta=\boldsymbol{\Delta}P/P, \tag{23}$$

where $P$ is the magnitude of the particle momentum.

In this calculation, the atomic potentials (7) and (8) are used. The corresponding single scattering angles are[19]

$$\boldsymbol{\Delta}\theta=(Z_1Z_2e^2/aE)(\mathbf{r}/r)[0.6K_1(6r/a)+0.66K_1(1.2r/a)+0.105K_1(0.3r/a)] \tag{24}$$

for the Molière potential and

$$\boldsymbol{\Delta}\theta=(Z_1Z_2e^2/E)(\mathbf{r}/r^2)[1+(r/Ca)^2]^{-1} \tag{25}$$

for the Lindhard potential. $K_1$ is the first-order modified Bessel function of the second kind.

Evaluating each subsequent scattering in this way, the computer then calculates the particle path. A Monte Carlo routine is used to synthesize the thermal vibration of the string atoms according to Eq. (3).

TABLE I. Calculated angular widths for 400-keV protons in [100] W ($d=3.16$ Å; $\psi_1=2.35°$; standard potential).

| Temp. (°K) | Vibration amplitude $\rho$ Å | Binary-collision model (all atoms vibrating) | Binary-collision model (single atom vibrating) | Halfway-plane model | Continuum model | $\rho/d\psi_1$ |
|---|---|---|---|---|---|---|
| Static | 0 | $3.2_0$ | $3.2_0$ | $3.3_0$ | | 0 |
| 0 | 0.036 | $2.7_0$ | $2.8_0$ | $2.8_0$ | $3.2_0$ | 0.55 |
| 300 | 0.071 | $2.2_5$ | $2.4_0$ | $2.4_5$ | $2.6_0$ | 1.08 |
| 900 | 0.122 | $1.9_0$ | $2.0_0$ | $2.0_5$ | $2.0_5$ | 1.86 |

[19] J. A. Brinkman, J. Appl. Phys. **25**, 961 (1954).

TABLE II. Calculated angular widths for 7-MeV protons in [110] Si ($d=3.8$ Å; $\psi_1=0.22°$; standard potential).

| Temp. (°K) | Vibration amplitude $\rho$ Å | Binary-collision model (all atoms vibrating) | Binary-collision model (single atom vibrating) | Halfway-plane model | Continuum model | $\rho/d\psi_1$ |
|---|---|---|---|---|---|---|
| Static | 0 | $0.47_0$ | $0.47_0$ | $0.47_0$ | | 0 |
| 0 | 0.069 | $0.27_5$ | $0.29_0$ | $0.28_5$ | $0.28_5$ | 5.2 |
| 300 | 0.108 | $0.23_5$ | $0.25_0$ | $0.25_0$ | $0.25_0$ | 8.1 |
| 900 | 0.179 | $0.18_5$ | $0.20_0$ | $0.20_0$ | $0.20_0$ | 13.4 |

## COMPARISON OF RESULTS

In the following, the results of various calculations are compared in two standard cases, 400-keV protons emitted from a ⟨100⟩ string in W and 7-MeV protons emitted from a ⟨110⟩ string in Si. These two cases were chosen partly to correspond to available experimental data, and partly to represent two energy regions, medium and high energies, defined by $\psi_1 \simeq \rho/d$ and $\psi_1 < \rho/d$, respectively [see Eq. (11)].

### Models

In order to compare the three different models, the binary-collision model, the halfway-plane model, and the continuum model, we compare the results obtained with the same representation of thermal vibrations. Only the emitting atom is allowed to vibrate. Also, the same average potential is used, Linhard's standard potential (5). Figure 3 shows calculations of the dip in emission yield in the tungsten case for $T=0$°K. The binary-collision calculation (I) and the halfway-plane calculation (II) are in excellent agreement. The shape of the shoulder is slightly different, but the widths agree within the accuracy of the calculations. The dip calculated in the continuum approximation (III), however, is quite different. The compensating shoulder is absent in this approximation, and the width is larger by ~14%.

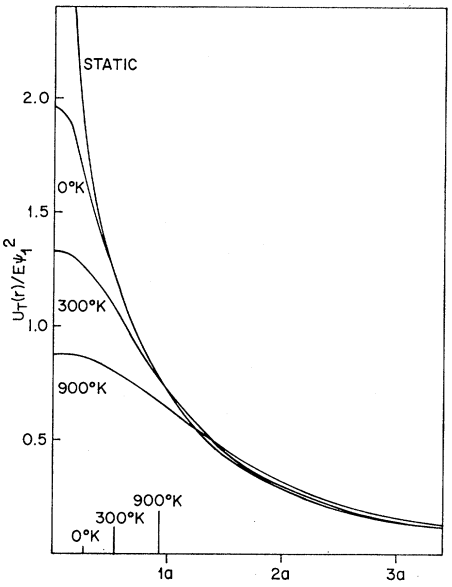


FIG. 7. Temperature-dependent average potentials for the [100] string in W.

This is not surprising, since the condition (II) for the validity of the continuum approximation is not fulfilled. In this case, we have $\rho/d\psi_1=0.55<1$.

Figure 4 shows the same calculation for the Si case at $T=300$°K. In this case, the three curves are indistinguishable. Condition (II) is fulfilled, since $\rho/d\psi_1=8.1>1$. A further comparison is given in columns 4, 5, and 6 of the Tables I and II.

In all cases, the widths obtained in the binary-collision model and in the halfway-plane model agree within accuracy. In the Si case, the same width is also obtained in the continuum model. It is interesting to note in the W case the improving accuracy of the continuum model for increasing values of $\rho/d\psi_1$.

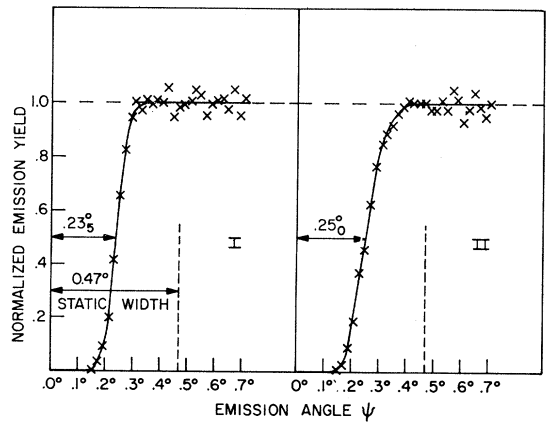


FIG. 6. Comparison of the calculated [100] dips in Si at 300°K for 7-MeV protons in the binary-collision model with (I) all atoms vibrating and (II) single atom vibrating.

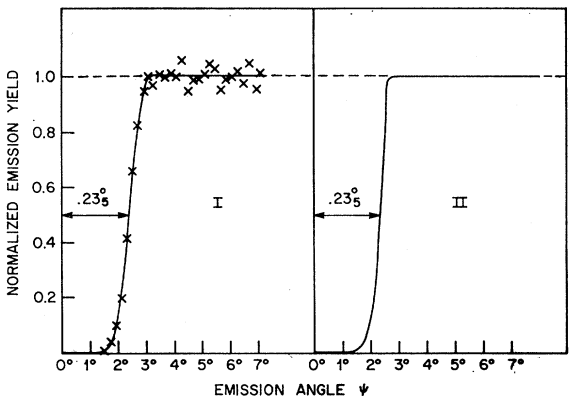


FIG. 8. Comparison of the calculated [110] dips in Si at 300°K for 7.0-MeV protons in the (I) binary-collision model with all atoms vibrating and (II) continuum model with a temperature-dependent average potential.

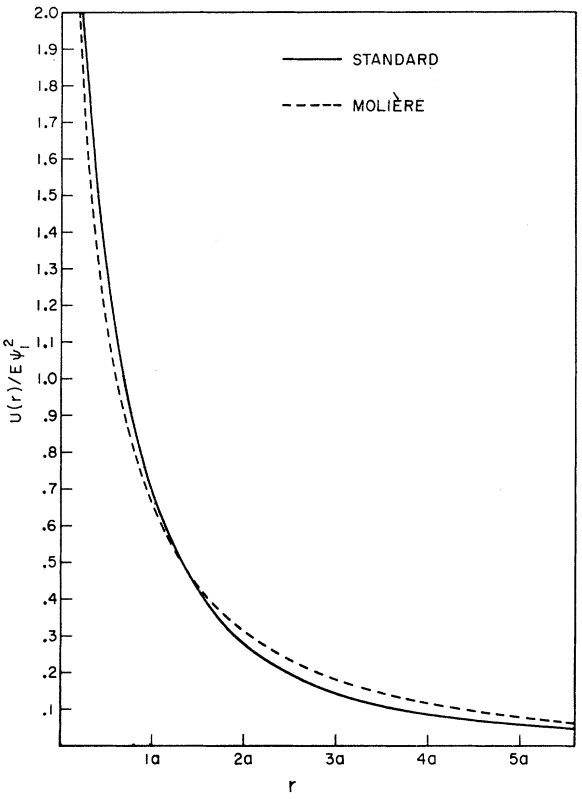


FIG. 9. Comparison of the standard (Lindhard) and Thomas-Fermi (Molière approximation) average potentials.

### Temperature Vibrations

In the binary-collision calculation, all string atoms may be allowed to vibrate. In Figs. 5 and 6, this type of calculation is compared to the single-atom vibration calculation in the two standard cases. The widths differ slightly, by ~3 and ~6%, respectively. The static width is also indicated in the figures, and it is seen that the influence of thermal vibrations on the angular width is mainly due to the vibration of the emitting atom.

A systematic comparison of widths at different temperatures in the two standard cases is given in Tables I and II. The difference between all atoms vibrating and the emitting atom only vibrating is ~5%, whereas the difference between the emitting atom only vibrating and the static case is a factor of ~2.

Although the vibrations of all atoms except the emitting atom have a small effect on the angular width, it may be interesting to see the influence of a more realistic temperature-dependent average potential on the continuum-model calculation. Figure 7 shows the [100] string potential in W, calculated on the basis of (18) for three different temperatures. The static-average potential is shown for comparison. According to (13), the width of the dip is, in the continuum description, determined by the value of the average potential at a distance $r=\rho\,(\ln 2)^{1/2}$. This distance is indicated at the bottom of Fig. 7 for the three different temperatures. It is qualitatively evident from this figure that the introduction of the temperature-dependent potential decreases $\psi_{1/2}$ by ~5%. Figure 8 compares the [110] Si dip as calculated in the binary-collision model with all atoms vibrating, and in the continuum model with a temperature-dependent potential, respectively. The two curves are indistinguishable (compare with Figs. 4 and 6). Thus, when the condition (II) is fulfilled, the vibrations of the string atoms may adequately be described by a combination of the vibration of the emitting atom and a temperature-dependent potential.

TABLE III. Calculated angular widths for 400-keV protons in ⟨100⟩ W ($T=300$°K).

| Potential | Binary-collision-model (all atoms vibrating) | Binary-collision model (single atom vibrating) | Halfway-plane model | Continuum model |
|---|---|---|---|---|
| Standard | $2.2_5$ | $2.4_0$ | $2.4_5$ | $2.6_0$ |
| Molière | $2.2_0$ | $2.3_0$ | $2.3_5$ | $2.4_5$ |

### Potential

Two different approximations to the Thomas-Fermi potential have been extensively used in channeling calculations, the Molière approximation (8) and the standard potential (7). The Molière approximation is a very accurate approximation to the Thomas-Fermi potential, whereas the standard potential, in many applications, is much more convenient, leading, e.g., to a simple analytical expression (14) in the continuum approximation. For a discussion of the accuracy of the standard potential, we refer to Ref. 17. The corresponding average string potentials are compared in Fig. 9. In Tables III and IV, half-widths of the calculated string dips for $T=300$°K are given for both potentials. Again, the differences are only ~5%.

## CONCLUSIONS

In general, the three different models are in good agreement. The continuum model, the halfway-plane description, and the binary-collision model may be thought of as steps towards a more realistic picture at the expense of ease of calculation and, perhaps, physical insight. The binary-collision model appears to represent

TABLE IV. Calculated angular widths for 7-MeV protons in [110] Si ($T=300$°K).

| Potential | Binary-collision model (all atoms vibrating) | Binary-collision model (single atom vibrating) | Halfway-plane model | Continuum model |
|---|---|---|---|---|
| Standard | $0.23_5$ | $0.25_0$ | $0.25_0$ | $0.25_0$ |
| Molière | $0.22_0$ | $0.23_5$ | $0.23_5$ | $0.23_5$ |

the most complete model in which all the string atoms are allowed to vibrate and the use of an average potential need not be enforced. It does contain as possible sources of error the assumptions in choice of potential and the model of thermal vibrations. These assumptions are intrinsic to all the models discussed in this paper. In addition, the validity of a classical binary-collision treatment of correlated scattering by string atoms can only be inferred from the results of Lindhard *et al.*,[17] who showed that at high particle velocities classical mechanics is applicable in the continuum model or halfway-plane description.

As we have shown, the vibration of the emitting atom is the most important thermal effect. Choosing to hold all atoms but the first fixed does not greatly simplify the binary-collision model but does permit the use of the halfway-plane description, a large simplification under these circumstances. The half-width of the dip $\psi_{1/2}$ is in this model close to $\psi_1$ given by (16), and the ratio $\psi_{1/2}/\psi_1$ is a function of two parameters only,[7] $\rho/a$ and $a/d\times\psi_1$. The agreement between the binary-collision model and the halfway-plane description with the same representation of thermal vibrations gives further justification for the use of an average potential. The all-atom vibration case may be treated in this description by the use of a temperature-dependent average potential but, again, at the expense of complexity of calculation.

The binary-collision model may give more detailed information about the scattering. Information about the number of string atoms effectively contributing to the steering may be of importance, especially in surface studies.[20] Also, complicated compound crystals may be studied by this method. Finally, different models of temperature vibrations may be incorporated in order to include correlations, etc.

For $\rho/d\times\psi_1>1$, the continuum model is in good agreement with the other two calculations. In this case, it represents the simplest prediction of the channeling angular distribution. The width of the dip in this picture is exactly proportional to $\psi_1$, and the factor of proportionality is a function of one parameter only, $\rho/a$. The half-width at half-dip, $\psi_{1/2}$, is determined by the average potential at the distance $r=\rho\,(\ln 2)^{1/2}$ from the string, as expressed in Eq. (13). When Lindhard's standard potential is inserted, a simple analytical expression for the distribution (14) as well as the width (15) is obtained.

[20] E. Bogh, Phys. Rev. Letters **19**, 61 (1967).

### Comparison with Experiments

We do not here intend to make any exhaustive comparison with experiments A large amount of data has been accumulated by several groups, and some of this data has been compared to calculations. In Refs. 7 and 21–23, experimental half-widths were compared to the results of a halfway-plane treatment, or the results of the continuum approximation [Eq. (15)]. In Ref. 11, the experimental data was compared to results of a binary-collision–model calculation. A few results of this type of calculation were also given in Ref. 21. In general, the agreement is rather good, i.e., the differences are $\lesssim 20\%$. The experimental values for the half-width, however, are consistently somewhat smaller than those calculated. This may partly be due to errors in the treatment of the interaction potential and thermal vibrations. Most likely also, the influence of planar effects on the measured axial dip contributes significantly to this discrepancy (see, e.g., Fig. 5, Ref. 24). Of special interest in this connection are calculations including the complete lattice structure.[13] Such calculations, however, are very time consuming, and no comparison with calculations of the type discussed in this paper has been made. A comparison to experimental data[25] showed a similar agreement as mentioned above.

A few comparisons between experimental result and the result of a simple two-body calculation have been made. Oen[10] succeeded in fitting the data by Domeij[26] rather well, but the fit was obtained for a rather small value of the vibrational amplitude. The two-body model should only be applicable at rather low energies (see Ref. 11). This is confirmed by the data on low-energy proton scattering from copper in Ref. 24.

A final point may be made. In Ref. 23, the simplest treatment of thermal vibrations (one atom vibrating) was shown to give a good account of the measured variations in the ratio $\psi_{1/2}/\psi_1$ due to differences in vibrational amplitude between various diamond-structure materials. The measured half-widths of the axial dip in these different crystals, however, were all too small by $\sim 25\%$ compared to Eq. (15).

[21] J. A. Davies, J. Denhartog, and J. L. Whitton, Phys. Rev. **165**, 345 (1968).
[22] J. U. Andersen and E. Uggerhoj, Can. J. Phys. **46**, 517 (1967).
[23] S. T. Picraux, J. A. Davies, L. Eriksson, N. G. E. Johansson, and J. W. Mayer, Phys. Rev. **180**, 873 (1969).
[24] R. Behrisch, Can. J. Phys. **46**, 527 (1967).
[25] T. S. Noggle and J. H. Barrett, Brookhaven National Laboratory Report No. BNL 50083 (C-52) (Physics TID-4500) (unpublished).
[26] B. Domeij and K. Bjorkquist, Phys. Letters **14**, 127 (1965).